A 106 Gb/s 2.5 V_{ppd} Linear Microring Modulator Driver with Integrated Photocurrent Sensor in 28nm CMOS

Hao Li, Meer Nazmus Sakib, Duanni Huang, Ranjeet Kumar, Haisheng Rong, Ganesh Balamurugan, and James Jaussi
Intel Corporation, USA
hao1.li@intel.com

Abstract: A low-power CMOS linear driver IC, optimized for microring modulator-based co-packaged optics, is presented. This 2.5 V_{ppd} driver, assembled with a photonic IC, achieves 2 dB TDECQ at 106 Gb/s PAM4 with 1.33 pJ/bit efficiency.

1. Introduction

Bringing photonics closer to network and compute silicon (e.g., switch, XPU, FPGA) – from faceplate pluggable modules to Co-Packaged Optics (CPO) – provides simultaneous improvements in bandwidth (BW) density and power efficiency to meet the needs of next-gen data center and high-performance computing applications [1]. Owing to their small footprint, silicon photonic microring modulator (MRM) is a key enabler for high BW density in CPO. As shown in Fig. 1(a), multiple MRM-based CPO tiles can be directly attached to a HOST IC to allow for an ultra-low-loss die-to-die interconnect from the HOST IC to each CMOS linear MRM driver. Although high-swing differential drivers have been widely adopted for travelling-wave MZM-based solutions (Fig. 1(b)), their use to drive depletion-mode MRMs presents two challenges: (a) the PN junction in MRMs require ~2-3 V reverse bias for optimal modulator performance [2] and (b) an integrated MRM photocurrent sensor is necessary for MRM thermal control [3]. Previously, AC-coupled differential MRM drivers with on-chip bias-T have been demonstrated to decouple the RF signal from DC bias [2-3] (Fig. 1(b)). However, due to the limited values realizable with integrated coupling capacitors, these designs require large (>100 kΩ) bias resistors to mitigate DC-wander for long run-length patterns. The MRM photocurrent can be >100 µA with high input laser power, resulting in >10 V voltage drop that requires impractical supply rails to maintain an effective junction reverse bias.

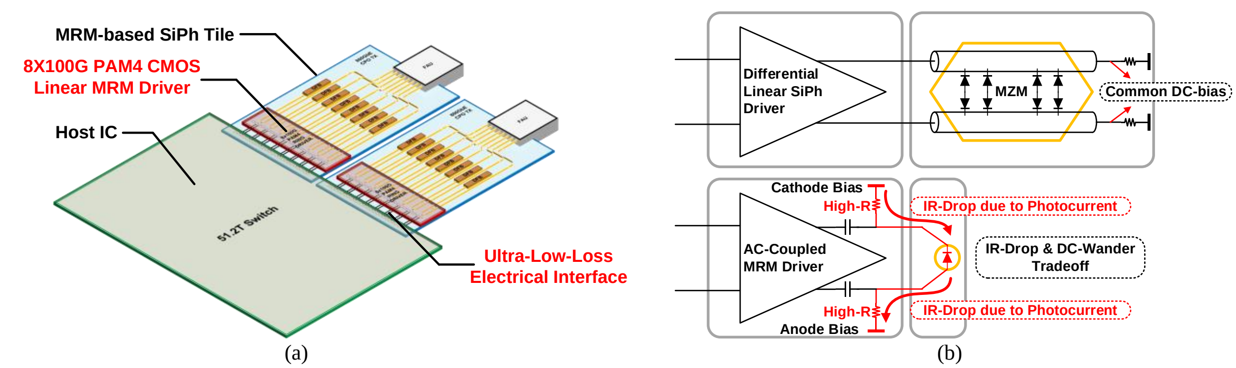

Fig. 1. (a) Conceptual view of MRM-based CPO TX. (b) Prior differential MZM driver and AC-coupled MRM driver.

In this work, we address this issue using a novel low-power CMOS linear driver with an auxiliary drive path that decouples the bias resistor value and driver low frequency cutoff. The proposed driver was designed to directly drive an MRM without the need of off-chip passive components. A photocurrent sensor was implemented to extract the MRM photocurrent for wavelength stabilization without an additional monitor PD or power monitor overhead.

2. Linear MRM Driver Architecture and Circuits

Fig. 2(a) shows the architecture of the proposed CMOS linear MRM driver. It consists of a main drive path and an auxiliary drive path with an integrated photocurrent sensor. The main driver output is AC-coupled to the MRM through an on-chip RC bias-T network. The auxiliary driver is DC-coupled to the anode and cathode of the MRM. Its output swing is matched to the main drive path to restore the low-frequency gain below the RC bias-T high-pass corner. Due to this auxiliary path, the bias-T resistance can be reduced by >100X to resolve the large photocurrent-induced voltage drop issue. As shown in Fig. 2(b), the main driver consists of a pseudo-differential stacked push-pull output stage to deliver 2.5 V_{ppd} output swing while satisfying the electrical overstress requirements. Inverter-based cherry-hooper amplifiers are used as the pre-driver for both PMOS and NMOS input to enhance the BW. The nominal driver gain is 17 dB. The electrical 3-dB BW is 40 GHz with a 50 fF MRM loading and 150 pH driver-MRM wire-bond inductance. The driver gain and BW can be adjusted to optimize the E-O response for specific MRM device and packaging parasitics.

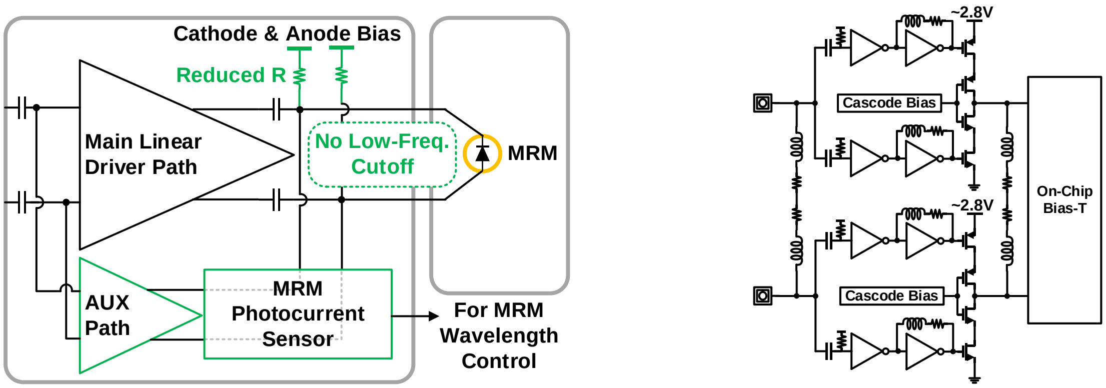

(a) (b)

Fig. 2. (a) Architecture of linear MRM driver. (b) Main driver circuit design.

3. Optical Measurement Results

A single channel driver prototype was fabricated in 28nm CMOS. The experiment setup used to characterize the driver IC is shown in Fig. 3. The driver IC was packaged onto an evaluation PCB with a companion photonic IC (PIC). The PIC consists of an on-chip O-band DFB laser and an MRM with 10 µm radius and ~3500 Q. A 120 GS/s AWG was used to generate 106 Gb/s PRBS15 PAM4 pattern as the optical TX (OTX) input. The OTX output was free-space coupled into a 40 GHz optical sampling scope after a 90/10 fiber splitter without additional optical amplifiers. The MRM resonance wavelength was controlled manually by adjusting the MRM heater power.

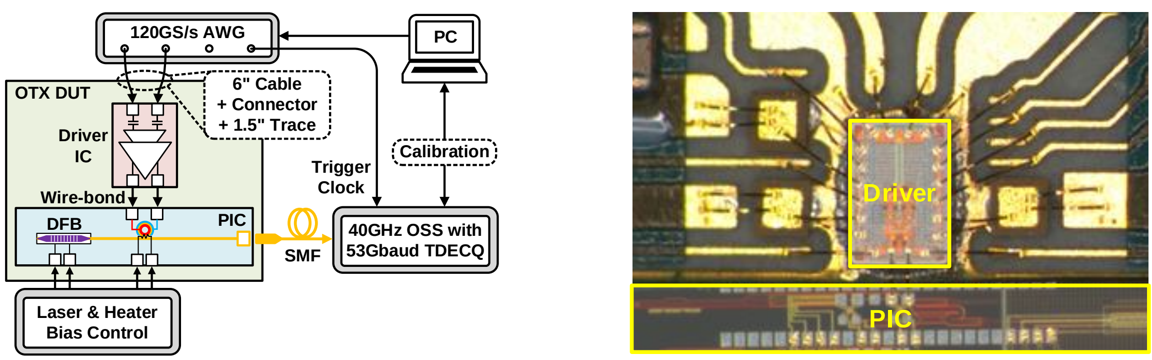

(a) (b)

Fig. 3. (a) Experiment setup for driver optical test. (b) Micrograph of the driver and PIC wire-bond assembly.

Fig. 4 shows the measured 106 Gb/s PAM4 optical eye-diagrams with 2.5 V_{ppd} modulation. Figure 4(a) was captured before calibrating the OTX E-O response. MRM detuning and reverse bias voltage were chosen to balance MRM nonlinearities and OMA [2]. The driver BW was adjusted to compensate for the RF connector and PCB trace insertion loss. The measured 3-dB E-O BW was 37 GHz based on the AWG in-system calibration result. Figure 4(b) shows the PAM4 eye with 10-tap scope FFE to compensate for residual ISI. The post-FFE TDECQ was 2 dB and OMA was -0.4 dBm (4 dB estimated insertion loss between the MRM and OSS). Figure 4(c) shows the measured PAM4 eye after calibrating the E-O response up to 45 GHz using the AWG DSP. The measured TDECQ after the E-O response calibration was 1.5 dB.

Figure 5(a) shows the output of the integrated photocurrent sensor, measured when sweeping the MRM resonant wavelength at two different laser power and MRM bias conditions. With 10 dBm input laser power and 3 V MRM bias, the maximum MRM photocurrent was 170 µA. The measured photocurrent curves match well with the MRM behavior in the presence of self-heating effect [4]. Figure 5(b) shows the effectiveness of the auxiliary path for DC-wander compensation. A lower baud rate (20 Gb/s) is used for this measurement in order to emphasize the DC-wander effect. A peak SNR of 16 can be achieved with matched gains between the main path and the auxiliary path. The driver IC achieves an energy efficiency of 1.33 pJ/bit at 106 Gb/s with only 8.3% of the power consumed by the auxiliary path.

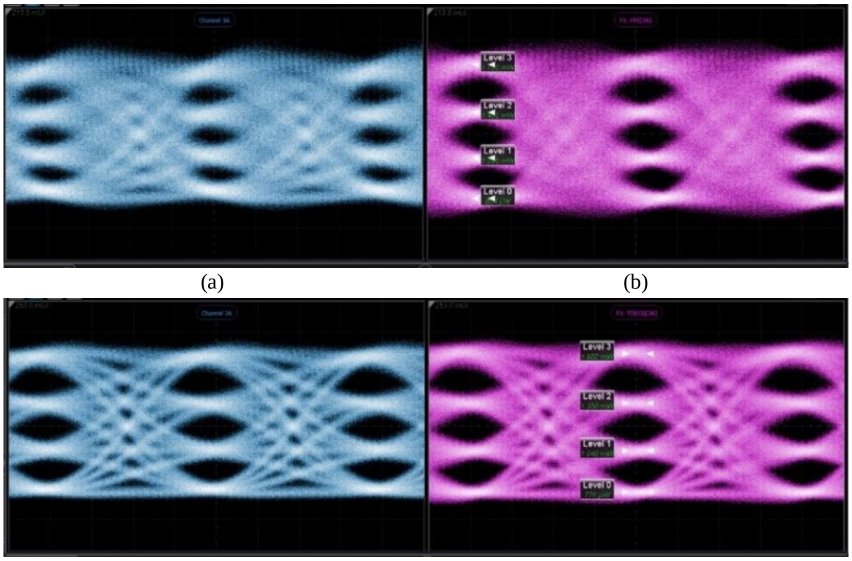

(a) (b)

(c) (d)

Fig. 4. Measured 106 Gb/s PRBS15 PAM4 eye-diagrams (a) without E-O calibration, (b) with 10-tap scope FFE, (c) with E-O calibration, and (d) with E-O calibration and 5-tap scope TDECQ filter.

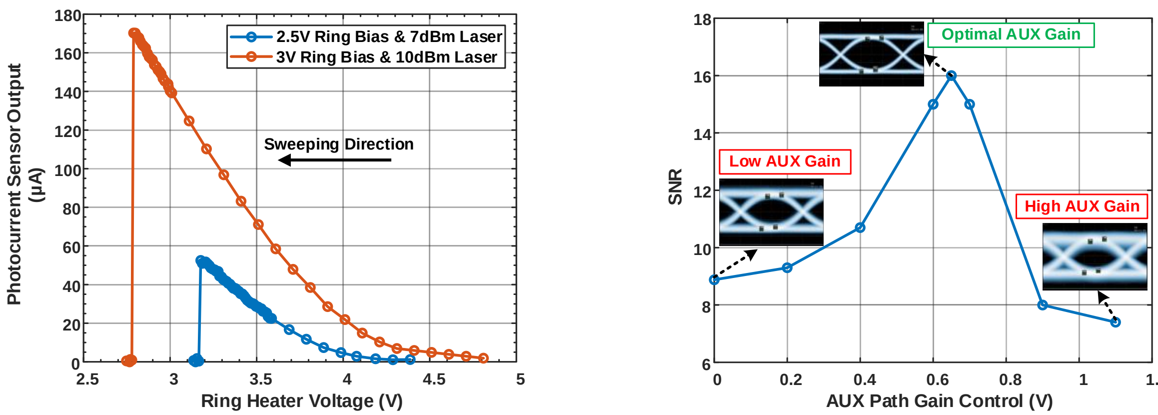

(a) (b)

Fig. 5. (a) Measured driver photocurrent sensor output versus ring heater voltage. (b) Measured 20 Gb/s NRZ PRBS15 SNR with different auxiliary path gain settings.

4. Conclusions

We have demonstrated a low-power CMOS linear MRM driver that is well-suited for high-density and low-power co-packaged optics. The driver design features an integrated photocurrent sensor and a dual-path architecture to drive an MRM directly with minimal DC-wander. The proposed driver IC delivers 2.5 V_{ppd} modulation voltage and achieves 2 dB optical TDECQ at 106 Gb/s with 1.33 pJ/bit energy efficiency.

5. Acknowledgement

The authors thank Chaoxuan Ma, Peicheng Liao for technical discussions, Suzuki Satoshi, Denise Souza for PCB design, and Intel Fab11x for high-quality PIC fabrication.

6. References

[1] S. Fathololoumi, *et al*., "1.6Tbps Silicon Photonics Integrated Circuit for Co-Packaged Optical-IO Switch Applications," OFC (2020).
[2] H. Li, *et al*., "A 112 Gb/s PAM4 Silicon Photonics Transmitter with Microring Modulator and CMOS Driver," JLT (2020).
[3] J. Sharma[ECA], H. Li[ECA], *et al*., "Silicon Photonic Micro-Ring Modulator-based 4 x 112 Gb/s O-band WDM Transmitter with Ring Photocurrent-based Thermal Control in 28nm CMOS," VLSIC (2021).
[4] C. Sun, *et al*., "A 45 nm CMOS-SOI Monolithic Photonics Platform With Bit-Statistics-Based Resonant Microring Thermal Tuning," JSSC (2016).